Neuro-Oncology

M011L-deficient oncolytic myxoma virus induces apoptosis in brain tumor-initiating cells and enhances survival in a novel immunocompetent mouse model of glioblastoma

Alexandra Pisklakova[†], Brienne McKenzie[†], Franz Zemp, Xueqing Lun, Rajappa S. Kenchappa, Arnold B. Etame, Masmudur M. Rahman, Karlyne Reilly, Shari Pilon-Thomas, Grant McFadden, Ebba Kurz, and Peter A. Forsyth

Department of Neuro-Oncology and Tumor Biology, Moffitt Cancer Center, Tampa, Florida (A.P., R.S.K., A.B.E., P.A.F.); Southern Alberta Cancer Research Institute, University of Calgary, Calgary, Alberta, Canada (B.M., F.Z., X.L., E.K., P.A.F.); Department of Molecular Genetics and Microbiology, University of Florida, Gainesville, Florida (M.M.R., G.M.); Center for Cancer Research, National Cancer Institute, Bethesda, Maryland (K.R.); Department of Immunology, Moffitt Cancer Center, Tampa, Florida (S.P.-T.)

Corresponding Author: Peter A. Forsyth, MD, Department of Neuro-Oncology, H. Lee Moffitt Cancer Center and Research Institute, 12902 Magnolia Drive Tampa, FL 33612 (peter.forsyth@moffitt.org).

[†]These authors contributed equally to this work.

Current Address: B.M.: 6-11 Heritage Medical Research Centre, Department of Medical Microbiology and Immunology, University of Alberta, Edmonton, T6G 2R3.

Background. Myxoma virus (MYXV) is a promising oncolytic agent and is highly effective against immortalized glioma cells but less effective against brain tumor initiating cells (BTICs), which are believed to mediate glioma development/recurrence. MYXV encodes various proteins to attenuate host cell apoptosis, including an antiapoptotic Bcl-2 homologue known as M011L. Such proteins may limit the ability of MYXV to kill BTICs, which have heightened resistance to apoptosis. We hypothesized that infecting BTICs with an M011L-deficient MYXV construct would overcome BTIC resistance to MYXV.

Methods. We used patient-derived BTICs to evaluate the efficacy of M011L knockout virus (vMyx-M011L-KO) versus wild-type MYXV (vMyx-WT) and characterized the mechanism of virus-induced cell death in vitro. To extend our findings in a novel immunocompetent animal model, we derived, cultured, and characterized a C57Bl/6J murine BTIC (mBTIC0309) from a spontaneous murine glioma and evaluated vMyx-M011L-KO efficacy with and without temozolomide (TMZ) in mBTIC0309-bearing mice.

Results. We demonstrated that vMyx-M011L-KO induces apoptosis in BTICs, dramatically increasing sensitivity to the virus. vMyx-WT failed to induce apoptosis as M011L protein prevented Bax activation and cytochrome *c* release. In vivo, intracranial implantation of mBTIC0309 generated tumors that closely recapitulated the pathological and molecular profile of human gliomas. Treatment of tumor-bearing mice with vMyx-M011L-KO significantly prolonged survival in immunocompetent—but not immunodeficient—mouse models, an effect that is significantly enhanced in combination with TMZ.

Conclusions. Our data suggest that vMyx-M011L-KO is an effective, well-tolerated, proapoptotic oncolytic virus and a strong candidate for clinical translation.

Keywords: apoptosis, brain tumor-initiating cells, glioma, oncolytic virus.

Glioblastoma is a deadly brain cancer with an average prognosis of 12–15 months.[1] Standard of care therapy includes surgery, radiation, and chemotherapy with temozolomide (TMZ), but long-term survival is rare.[1] Recurrence is believed to be driven by a treatment-resistant, stem cell-like compartment.[2,3] These brain tumor-initiating cells (BTICs) have been isolated from glioma surgical samples and cultured under neural stem cell-promoting conditions[4] that maintain the "stem-like" nature of gliomas in vitro and in vivo[5] and provide a valuable model for evaluating glioblastoma therapies.

Oncolytic virus (OV) therapy utilizes replication-competent viruses with a specific tropism for cancer cells. OVs are thought to be multimodal, directly killing tumor cells while simultaneously activating a robust inflammatory response that promotes

antitumor immunity.[6,7] Clinical responses to OVs have been observed in glioma patients, with no significant safety or toxicity issues.[8] However, the failure to achieve durable responses suggests that existing viruses may not be sufficiently effective against the highly resistant BTIC compartment.

Myxoma virus (MYXV) is a potent OV with significant efficacy in preclinical glioblastoma models.[9–11] Efficacy in patient-derived BTICs is less robust than in immortalized glioma cell lines. We recently addressed this issue by sensitizing BTICs to MYXV-mediated cell death pharmacologically.[9,12] In investigating alternative strategies for enhancing cell killing, we hypothesized that sensitizing BTICs to apoptosis would enhance OV efficacy. Utilizing a MYXV construct that induces apoptosis is an attractive strategy since BTICs are intrinsically resistant to apoptosis and express high levels of antiapoptotic proteins.[13]

Apoptosis is a highly effective viral evasion mechanism.[14] Following infection, activation of host proapoptotic Bcl-2 proteins initiates mitochondrial events culminating in Bax- and Bak-mediated permeabilization of the mitochondrial membrane and the release of cytochrome *c* into the cytoplasm.[15] This activates effector caspases (3,6, and 7), which shut down transcription and translational machinery.[15] Inhibition of transcription and translation early in apoptosis prevents this machinery from being hijacked by replicating viruses.[14,16] To circumvent this, many viruses encode antiapoptotic proteins.[15] MYXV encodes several viral proteins that attenuate cell death,[15,17] the best characterized of which is M011L,[17] a structural mimic of the antiapoptotic host protein Bcl-2.[18] Upon expression in immortalized cell lines, M011L interacts with the mitochondrial membrane permeability pore and inhibits cytochrome *c* release.[19] Subsequent studies found that M011L sequesters the proapoptotic cellular proteins Bak and Bax to block apoptosis.[20] We hypothesized that infecting BTICs with a MYXV construct lacking the antiapoptotic protein M011L (vMyx-M011L-KO) would enhance virus-mediate BTIC killing through induction of apoptosis.

To test this hypothesis, we utilized the vMyx-M011L-KO construct in human and murine BTICs in vivo and in vitro. We report that vMyx-M011L-KO efficiently kills patient-derived BTICs through caspase-dependent apoptosis. We also derived a novel murine BTIC line from a spontaneous high-grade glioma (developed in Trp53$^{+/-}$ Nf1$^{+/-}$ C57Bl/6J mice).[21] Treatment of mBTIC tumors with vMyx-M011L-KO significantly prolonged survival and acted in combination with TMZ to produce durable responses in immunocompetent animals. Given that the BTIC compartment is considered an important therapeutic target, our data suggest vMyx-M011L-KO as an ideal candidate for clinical translation.

Methods

Detailed protocols are included in the Supplementary Materials and Methods.

Cell Culture

Human BTIC lines (Table 1) were established from tissue samples obtained through the University of Calgary Neurologic and Pediatric Tumor and Related Tissue Bank. Mouse BTIC lines were derived from C57BL/6J NPcis mice.[21,22] BTICs were cultured in serum-free neural stem cell media with EGF, FGF, and heparin (Stem Cell Technologies) and differentiated using 10% fetal bovine serum (FBS) for 5–7 days.[9]

Stock Virus Titration and Viability Assays

Wild-type (WT) and knockout (KO) viruses were generated[23,24] and propagated[25] as described previously. Stock virus was titrated on baby green monkey kidney (BGMK) cells using plaque-forming assays.[25] BTIC viability was measured using Alamar Blue (described previously).[12]

Caspase 3/7 Activation Assays

Caspase 3/7 activity was measured using the Caspase-Glo 3/7 assay from Promega according to manufacturer's instructions.

Immunofluorescence, Immunohistochemistry, and Flow Cytometry

Immunofluorescent and immunohistochemical staining were performed using standard procedures. Purified rabbit anti-M011L was developed in G.F.'s laboratory. For fluorescence-activated cell sorting, cells were acquired using LSRII flow cytometer and analyzed using FlowJo software.

Immunoblotting

Preparation of whole-cell lysates and immunoblotting were conducted following standard protocols as described previously.[9]

Short Interfering RNA Transfection

BTICs were transfected with Bax short interfering RNA (siRNA) using Amaxa Mouse NSC Nucleofector Kit and program T-30 (Lonza).

In Vivo Studies

Experimental procedures were performed in accordance with USF IACUC guidelines. Tumor-bearing mice were intratumorally

Table 1. Genetic and molecular characteristic of BTIC25 and BTIC48 (modified from Kelly 2009 and Weiss 2013)

Id	Path	Growth	EGFR	CD15	CD133	CD271	Sox2	pAkt	Nestin	Mushasi-1	MGMT	P53	PTEN	TMZ	MYXV
BT025	GBM IV-r	Spheres	wt	−	−	+	+	low	+	+	M&U	T125R	G129R	R	S
BT048	GBM IV	Spheres	G598V	+	+	+	+	high	+	+	M	wt	wt	S	S

Abbreviations: BTIC, brain tumor-initiating cells; M, methylated; MYXV, Myxoma virus; Path, pathology; r, recurrent tumor; R, resistant; S, susceptible; TMZ, temozolomide; U, unmethylated; wt, wild-type.

treated with virus as described previously.[9] TMZ was administered intraperitoneally at 100 mg/kg for 5 days.

Results

Infection With vMyx-M011L-KO but not vMyx-WT Induces Apoptosis in BTICs

To determine whether knockout of antiapoptotic viral protein M011L improved MYXV efficacy, we treated 2 patient-derived BTICs (BTIC25 and BTIC48) with vMyx-WT or knockout virus vMyx-M011L-KO and measured BTIC viability using Alamar Blue (Fig. 1A). vMyx-M011L-KO caused a significantly greater reduction in cell viability than vMyx-WT in both BTIC25 and BTIC48. Cell death was validated using a Trypan Blue exclusion assay (Supplementary Material, Fig. S1), demonstrating a significant ($P < .05$) decrease in viable cell count in vMyx-M011L-KO-treated cultures compared with vMyx-WT and untreated controls. While healthy, multicellular neurospheres were observed in untreated and vMyx-WT-infected BTIC cultures, vMyx-M011L-KO-infected BTICs failed to form neurospheres (Fig. 1B). Killing of the non-BTIC glioma line U87, which is highly susceptible to vMyx-WT infection, was not significantly improved by infection with vMyx-M011L-KO (Supplementary Material, Fig. S2).

To determine whether the increased cytopathogenicity of vMyx-M011L-KO was due to increased viral infection, we evaluated viral protein expression with immunoblot analysis. Comparable levels of early viral protein MT-7 were detected in both BTIC lines, whereas M011L protein was detected only in vMyx-WT-infected BTICs as expected (Fig. 1C). To investigate whether differences in viral replication accounted for differences in viral efficacy, whole-cell titers were performed to quantify infectious progeny. vMyx-WT and vMyx-M011L-KO replicated with comparable efficiency in both BTIC25 and BTIC48 lines (Fig. 1D) and had comparable growth kinetics and replication capability on standard BGMK cells (Supplementary Material, Fig. S3).

We next examined caspases 3/7 activation at 48 hours post infection using a luminescent Caspase-Glo 3/7 assay. While vMyx-WT did not induce caspase 3/7 activation, vMyx-M011L-KO infection significantly increased caspase 3/7 activation at 1 and 10 multiplicity of infection (MOI; $P < .05$ and $P < .01$, respectively) (Fig. 1F). Induction of caspase activity was abrogated by co-treatment with pan-caspase inhibitor ZVAD ($P < .01$). Caspase activation was further examined via immunoblotting for the caspase 3 substrate, poly ADP-ribose polymerase (PARP). PARP cleavage was observed following vMyx-M011L-KO infection and doxorubicin treatment (positive control) but not following vMyx-WT infection (Fig. 1E). Flow cytometric quantification revealed that only doxorubicin and vMyx-M011L-KO increased cleaved caspase-3 (Fig. 1G). Collectively, these results demonstrated that apoptosis is induced in vMyx-M011L-KO-infected BTICs.

M011L Protein Localizes to Mitochondria in BTICs Infected With vMyx-WT and Prevents Apoptosis

Previous cell culture studies have demonstrated that Bax activation and cytochrome c release are inhibited by M011L.[26] To understand if this mechanism occurs in BTICs, we infected BTICs with vMyx-WT or vMyx-M011L-KO and utilized immunocytochemistry to assess subcellular localization of M011L, Bax, and cytochrome c.

In agreement with previous results,[26] M011L localized to the mitochondria in vMyx-WT-infected BTICs (Fig. 2A). As expected, no M011L staining was observed in MyxV-M011L-KO-infected or untreated cells (Supplementary Material, Fig. S4). Further, only vMyx-M011L-KO virus recruited Bax to the mitochondrial membrane. This is apparent as intense staining around the mitochondrial membrane using an activated Bax-specific antibody (clone 6A7).[27] This staining was absent in vMyx-WT-infected cells, suggesting that M011L inhibits Bax activation (Fig. 2B). Immunofluorescent staining for cytochrome c demonstrated its release into the cytoplasm following vMyx-M011L-KO infection (Fig. 2C) comparable to cells treated with doxorubicin, which stimulates cytochrome c release.[28] Cytochrome c release was not induced in BTICs infected with vMyx-WT (Fig 2C).

We next wanted to determine if Bax is required for apoptosis in vMyx-M011L-KO-infected BTICs. We utilized 2 Bax-specific siRNAs to downregulate its expression. BTICs were electroporated with either a control, nontargeting pooled siRNA or 1 of 2 Bax-specific siRNAs. Reduction of Bax expression was confirmed by immunoblotting (Fig. 2D). siRNA-transfected cells were infected with vMyx-WT or vMyx-M011L-KO, and caspase 3 activation was assessed by flow cytometry. Bax depletion decreased vMyx-M011L-KO-induced caspase 3 activation (Fig. 2E and Supplementary Material, Fig. S5). These results indicate that reducing host Bax expression attenuates vMyx-M011L-KO-induced apoptosis.

vMyx-M011L-KO Combined With TMZ Prolongs Survival and Produces Durable Responses in an Immunocompetent Orthotopic Syngeneic Murine Glioma BTIC Tumor Model

We first demonstrated that vMyx-M011L-KO was well-tolerated in vivo, with no neurobehavioral symptoms or loss of body weight in either naïve or BTIC48-bearing mice after intracranial infection (Supplementary Material, Fig. S6). We tested vMyx-M011L-KO versus vMyx-WT in human BTIC-implanted NOD SCID *gamma* (NSG) mice. These mice are severely immunocompromised as characterized by a lack of functional B and T cells, no natural killer cell activity, functionally immature macrophages and dendritic cells, a lack of complement activity, and cytokine signaling deficiencies.[29,30] Given that the induction of cell death can provide additional inflammatory stimuli, these experiments were designed to test the efficacy of the 2 viruses in vivo in the absence of potentially therapeutic inflammatory responses. Surprisingly, neither virus was capable of providing a survival benefit in the BTIC25 and BTIC48 models in NSG mice (Supplementary Material, Fig. S7A and B). This is in contrast to what we have previously shown in SCID mice, where vMyx-WT alone significantly improves survival.[9] SCID mice are not as immunocompromised as NSG mice, lacking mature B and T cells, while the innate immune responses are largely unaffected. This led us to believe that components of the innate immune response were important for mediating MYXV-treatment efficacy in orthotopically implanted BTICs. For this reason, we created a more relevant model for assaying immunotherapeutics: a novel immunocompetent murine BTIC model.
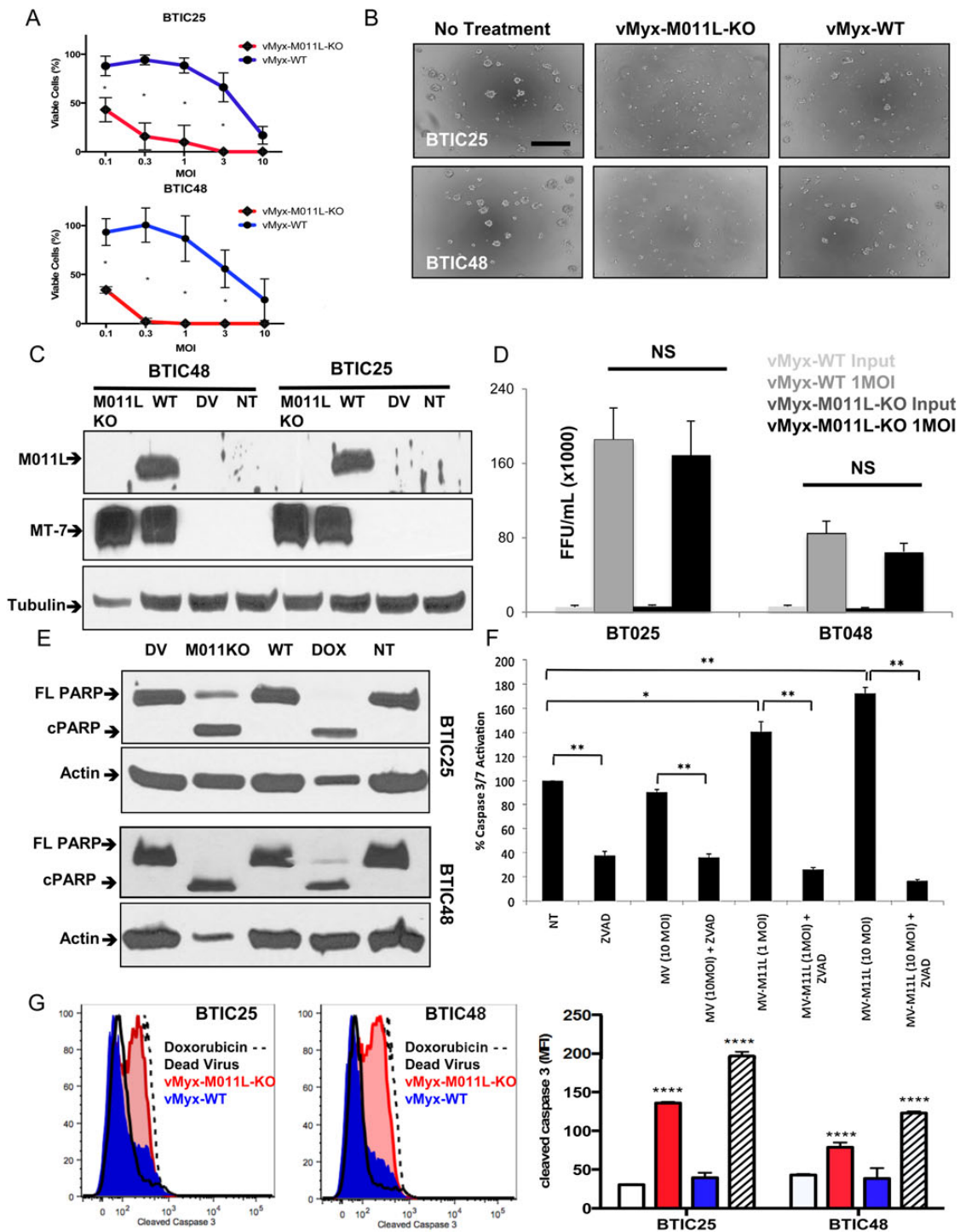
Fig. 1. Infection with Myxoma virus M011L knockout virus (vMyx-M011L-KO), but not vMyx-wild-type (WT), induces apoptotic cell death in brain tumor-initiating cells (BTICs) in vitro. (A) Viability assay (Alamar Blue) of BTIC25 and BTIC48 72 hours post infection with vMyx-WT or vMyx-M011L-KO. vMyx-M011L-KO kills BTICs significantly more effectively than vMyx-WT in both BTICs tested. Data shown are mean ± SEM of experiments performed in triplicate, and results represent at least 3 independent experiments (*; $P < .05$ by Student t test). (B) vMyx-M011L-KO-treated BTICs show substantial cytopathic effects compared with vMyx-WT treated cells. Neurospheres were imaged using a Zeiss Axiovert microscope at 20× magnification, 96 hours post infection. Scale bar, 100 μm. Data are representative of 3 independent experiments. (C) BTIC25 and BTIC48 cells were infected with vMyx-WT (10 multiplicity of infection [MOI]), vMyx-M011L-KO (10 MOI), UV-inactivated MYXV (dead virus, DV) or left untreated (NT) for 24 hours prior to preparation of whole cell extracts. Extracts were immunoblotted for M011, MT-7 (early viral gene expression), and tubulin (protein loading control). (D) The number of viral progeny produced by infected BTICs was quantified by counting the number of foci-forming units (FFUs) found on baby green monkey kidney (BGMK) cells treated

Three murine BTIC (mBTIC) cell lines were developed from C57Bl/6J NPcis mice that spontaneously develop gliomas[21] (Supplementary Material, Fig. S8), known as mBTIC0309, mBTIC0528, and mBTIC1116. Initial pathology of parent murine tumors indicated that they recapitulated key features of a human WHO grade IV glioblastoma. Tumors were hypercellular, with atypical elongated-to-oval nuclei and coarse chromatin. There were frequent mitoses indicative of a high mitotic index, and the tumors were highly vascular with signs of neovascularization. There were limited signs of necrosis, and tumors were infiltrative into adjacent tissue (Supplementary Material, Fig. S8B). Following isolation and culture under neural stem cell-promoting conditions, mBTICs grew as neurospheres and underwent differentiation when cultured with 10% FBS (Supplementary Material, Fig. S9).

We chose mBTIC0309 for further characterization in vitro and in vivo. mBTIC0309 neurospheres under stem cell conditions expressed the pluripotency transcriptional factor SOX2 and the intermediate filament nestin, both associated with neural stem cells (Fig. 3A). In addition to pluripotency markers, most mBTIC0309 cells under stem cell conditions (>70% as measured by flow cytometry) express the transmembrane glycoprotein CD133 (Prominin-1), an important neural progenitor cell surface marker, and retinoic acid early precursor transcript (Rae-1δ, >90%), a ligand for the natural killer cell-activating receptor that is highly expressed in neuronal progenitor cells[31] (Fig. 3A). The ability to differentiate into multiple neural lineages was tested by culturing mBTIC0309 in 10% FBS for 5–7 days. We observed multilineage differentiation by microscopy (Fig 3A and Supplementary Material, Fig. S9) and confirmed by immunostaining for neuronal marker Tuj1, astrocyte marker GFAP and oligodendrocyte marker OLIG2. Differentiation of mBTIC0309 resulted in diminished expression of CD133 and Rae-1δ, as confirmed by flow cytometry, and both SOX2 and nestin, as confirmed by immunostaining (Supplementary material, Fig. S9). Dramatically reduced expression of CD133 and Rae-1δ was observed under growth factor deprivation conditions (Supplementary Material, Fig. S9A II). In addition, these mBTIC cells lacked expression of MHC I and co-stimulatory molecules CD80, CD40 and CD86 (Supplementary Material, Fig. S9).

Following intracranial implantation of mBTIC0309 into C57Bl/6 mice, we observed the formation of large, heterogeneous, infiltrative tumors that recapitulated human gliomas. These mBTIC tumors expressed markers for progenitor cells (nestin) as well as differentiated cells including endothelial cells (CD31), oligodendrocytes (OLIG2), and astrocytes (GFAP; Fig. 3B). This suggests the persistence of the stem-like compartment within the more differentiated tumor environment, recapitulating human glioblastomas.

In vitro, we found that mBTIC0309 was relatively resistant to infection with vMyx-WT, even at 10 MOI. However, mBTIC0309 was susceptible to vMyx-M011L-KO (Fig 3C and D). We found significant activation of caspase-3 in the vMyx-M011L-KO-infected, but not vMyx-WT-infected, mBTICs, suggesting that M011L effectively inhibits apoptosis in both human (Fig. 1) and murine (Fig 3F) BTICs.

To assess the efficacy of vMyx-M011L-KO in vivo, C57BL/6J mice were engrafted with mBTIC0309 and treated with one intratumoral dose of vMyx-WT, vMyx-M011L-KO, or UV-inactivated (dead) virus. Median survival of mice ($n = 5$/group) treated with vMyx-WT (39 days) was not different from the dead virus group (37 days, $P = .1$), whereas vMyx-M011L-KO treatment significantly prolonged survival (48 days; $P = .03$; 30% increase in median survival) compared with all treatment groups (Fig 4A; additional experiments shown in Supplementary Material, Fig. S10). To test if an intact innate immune response was necessary for vMyx-M011L-KO efficacy, we tested vMyx-M011L-KO and vMyx-WT in NSG mice bearing mBTIC0309 tumors. As with human BTICs, both viruses failed to provide significant survival advantage ($P = .3$) in immunocompromised animals (Fig 4B). These results demonstrated that the immune response to viral infection is necessary to mediate the therapeutic efficacy of this virus.

TMZ is the current clinical standard of care therapy for gliomas. We hypothesized that a combination of vMyx-M011L-KO and TMZ could increase apoptosis and kill mBTICs. Having shown that a combination of vMyx-M011L-KO with a clinically relevant dose of TMZ induces enhanced cell death and apoptosis in patient-derived and murine BTICs (Supplementary Material, Fig. S11) in vitro, we evaluated combination treatment in vivo using the syngeneic mBTIC model. Mice were engrafted with mBTIC0309 and treated with a single dose of virus as described above. Three days post infection, mice were treated with 100 mg/kg of TMZ for 5 consecutive days. Kaplan-Meier survival analysis revealed a significant increase in median survival of mice treated with vMyx-M011L-KO plus TMZ (60% of animals alive at 55 days) compared with either agent alone (37.5 days for vMyx-M011L-KO alone and 29 days, $P = .03$ for TMZ alone) or vMyx-WT (31 days, $P = .03$ for virus

with whole cell lysate from infected BTIC cultures. Titers were not significantly different between vMyx-M011L-KO and vMyx-WT in either BTIC25 or BTIC48. (E) PARP cleavage in BTICs induced by vMyx-M011L-KO. Cell extracts were prepared 48 hours post-infection with 10 MOI vMyx-M011L-KO, vMyx-WT, or UV-inactivated MYXV (DV) or doxorubicin treatment (10 μM; positive control). Full-length (FL) and cleaved (C) forms of poly ADP-ribose polymerase (PARP) were assessed by immunoblotting using actin as a loading control. The figure shown is representative of results observed in 3 independent experiments. (F) Activation of caspase 3/7 in vMyx-WT and vMyx-M011L-KO-treated BTIC25 in vitro. Caspase 3/7 activation was assessed using Promega Caspase-Glo 3/7 assay. Luminescence is proportional to active caspase 3/7 in the sample, and was normalized to untreated BTIC25 (NT). Specificity of the assay for caspases was confirmed using the pan-caspase inhibitor ZVAD, which inhibited both constitutively active and vMyx-M011L-KO-activated caspases. vMyx-M011L-KO virus induced caspase 3/7 activation at both low (1 MOI) and high concentrations (10 MOI) of virus, whereas vMyx-WT (10 MOI) did not induce caspase 3/7 activation beyond the level observed in untreated (NT) cells. The data are representative of 3 independent experiments, and error bars represent mean ± SEM. *$P < .05$; **$P < .01$ by 2-sided t test. (G) BTICs were infected with vMyx-M011L-KO (10 MOI), vMyx-WT (10 MOI), UV-inactivated (dead) virus, or treated with doxorubicin (10 μM). Cells were collected after 72 hours, fixed, and stained with an antibody specific for cleaved caspase 3 and analyzed by flow cytometry. Data are representative of 3 independent experiments. Means ± SD from triplicates are shown (****$P < .0001$ by ANOVA compared with dead virus).
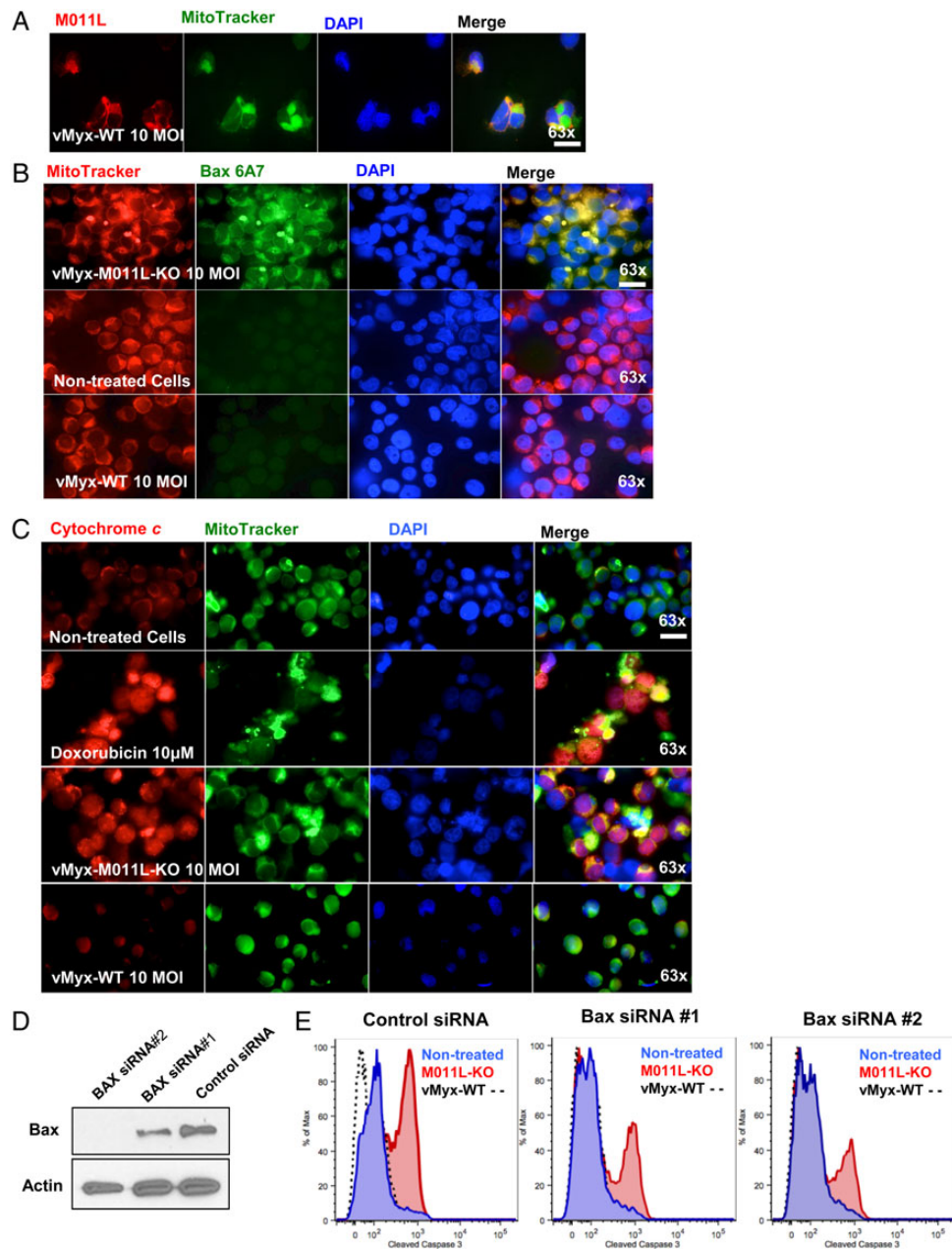
Fig. 2. M011L protein localizes to mitochondria in brain-tumor initiating cells (BTICs) infected with vMyx-WT and prevents cytochrome *c* release by associating with proapoptotic protein Bax. (A) BTIC25 cells were infected with vMyx-WT (10 multiplicity of infection [MOI] for 24 hours prior to co-staining for M011L, mitochondria (Mitotracker Green FM) and nuclei (DAPI). Cells were visualized using an automated Zeiss Observer Z.1 inverted microscope through a 63X/1.4NA objective. M011L protein shows mitochondrial localization in cells infected with vMyx-WT. The data are representative of 3 independent experiments. (B) BTIC48 cells were infected with vMyx-WT (10 MOI), vMyx-M011L-KO (10 MOI), or left untreated for 6 hours prior to staining with an Alexa Fluor 488-labeled antibody to Bax (clone 6A7), Mitotracker Red, and DAPI. Note the co-localization (yellow) of active Bax with the mitochondria following infection with vMyx-M011L-KO (row 1, panel 4). Data represent 3 independent experiments. (C) BTIC48 were infected with vMyx-WT (10 MOI), vMyx-M011L-KO (10 MOI), treated with doxorubicin (10 μM) or left untreated for 10 hours prior to co-staining for cytochrome *c* (Alexa Fluor 546, red), mitochondria (MitoTracker Green FM), and nuclei (DAPI). Note increased staining for cytochrome *c* in cytosol (yellow) following treatment with doxorubicin (row 2, panel 4) and vMyx-M011L-KO (row 3, panel 4). Scale bar 25 μm. (D) BTIC48 cells were transfected with siRNAs specific for Bax or a control nontargeting pooled siRNA. After 48 hours, cells were collected, and Bax expression was determined by immunoblotting. (E) In parallel, 48 hours after transfection with siRNAs, BTICs were infected for 72 hours with either vMyx-M011L-KO (10 MOI), vMyx-WT (10 MOI), or left uninfected prior to assessing caspase 3 activation by flow cytometry.
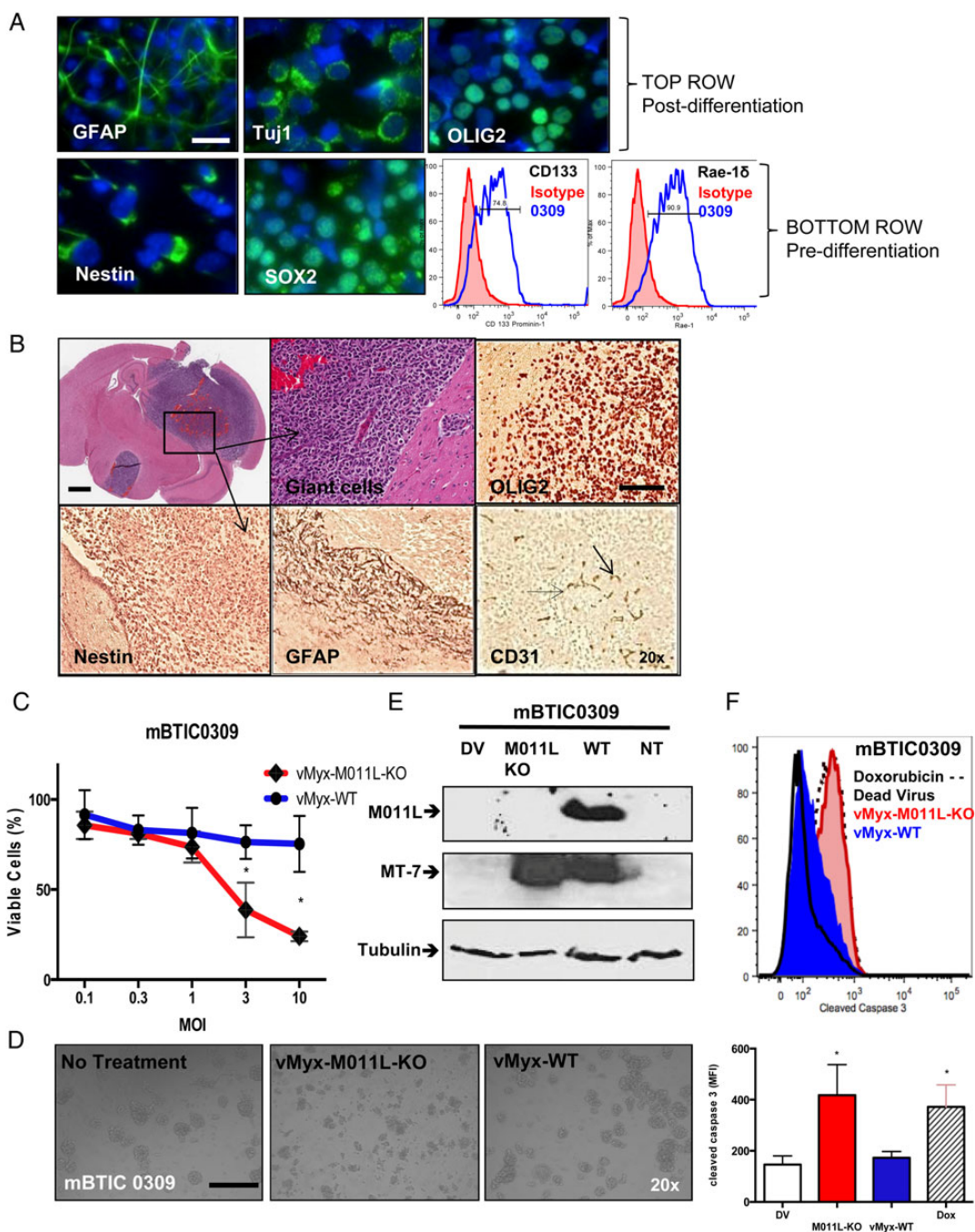
Fig. 3. Development and in vitro characterization of murine BTIC0309. (A) In vitro, neurospheres express neuronal markers SOX2, nestin, CD133 (Prominin-1) and Rae-1δ (NK-cell ligand, lower right fluorescence-activated cell sorting [FACS]) and can be differentiated in serum into glial (GFAP), neuronal (Tuj1), and oligodendrial (OLIG2) cell types. Scale bar 25 μm. (B) Mouse brain cross-section after intracranial implantation of mBTIC0309 at day 35 post infection. Scale bar 2 mm. Higher magnification of tumor tissue depicts cytonuclear pleomorphism and giant cells (upper middle). Tumors express endothelial cell marker CD31 and neuronal markers and maintain stem cell characteristics, as seen by immunohistochemistry of OLIG2, nestin and GFAP (brown staining) Scale bar 200 μm. (C) Alamar Blue assay of mBTIC0309 72 hours after infection with vMyx-WT or vMyx-M011L-KO. Data are mean±SEM of experiments performed in triplicate, and results are representative of at least 3 independent experiments (*; $P < .05$ by Student t test). (D) vMyx-M011L-KO-treated mBTIC0309 shows substantial evidence of cytopathic effects compared with vMyx-WT treated cells. Neurospheres were imaged using a Zeiss Axiovert microscope at 20× magnification, 72 hours post infection. Data represent 3 independent experiments. (E) Immunoblot 24 hours after vMyx-WT or vMyxV-M011L-KO infection for M011L, MT-7 (early viral gene expression), and tubulin (protein loading control). (F) mBTIC0309 were infected with vMyx-M011L-KO (10 MOI), vMyx-WT (10 MOI), or UV-inactivated (dead) virus or treated with doxorubicin (10 μM). Cells were collected after 72 hours, fixed, and stained with an antibody for cleaved caspase 3 and analyzed by flow cytometry. Data are representative of 3 independent experiments. Means±SD from triplicates are shown (*$P < .05$ by ANOVA compared with dead virus).
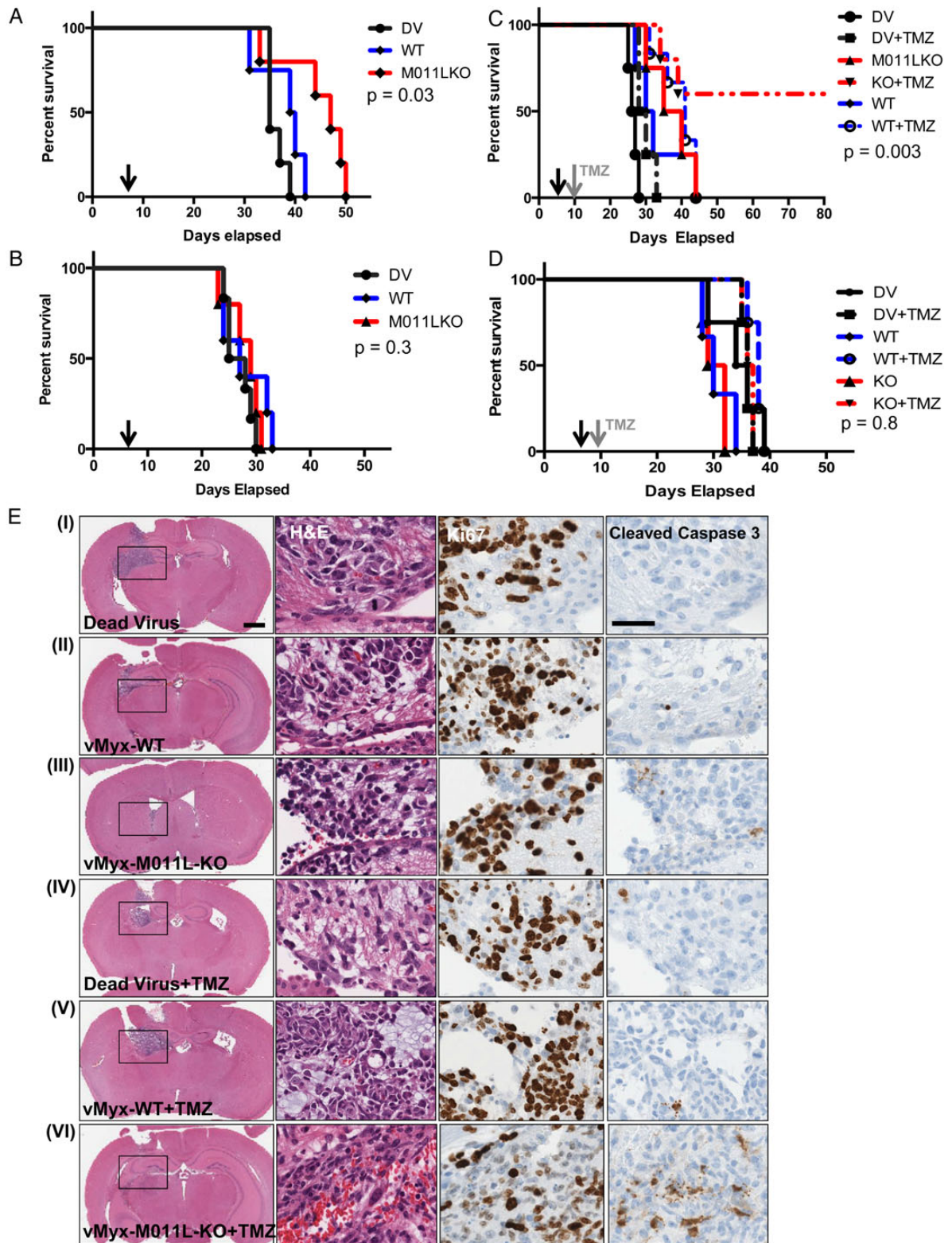
Fig. 4. vMyx-M011L-KO prolongs survival of immunocompetent mice bearing syngeneic gliomas and results in long-term survival in combination with temozolomide (TMZ). Kaplan-Meier survival curve of mBTIC0309-bearing immunocompetent C57BL/6 mice (A) or immunodeficient NOD SCID *gamma* mice (B) treated with 5×10^6 foci-forming units (FFUs) of vMyx-WT, vMyx-M011L-KO or UV-inactivated MYXV. Five mice were randomly assigned to each experimental group, and a single intratumoral virus injection was performed on day 7 after tumor implantation (black arrow). Statistical significance ($P = .03$, compared with vMyx-WT or dead virus, for C57BL/6J mice, (A) was determined using log-rank Mantel-Cox test.

alone and 41 days for combined treatment, $P = .008$) and UV-inactivated (dead) virus ($P = .003$, 26.5 days) (Fig. 4C). vMyx-M011L-KO, both alone and in combination with TMZ, was associated with an increase in $CD3^+$ cell infiltration (Supplementary Material, Fig. S12). To assess whether lasting adaptive antitumor immunity had been generated in the long-term survivors, we re-challenged "cured" animals ($n = 3$) with subcutaneous implantations of mBTIC0309 on day 65. We observed that subcutaneous mBTIC0309 tumors grew with similar kinetics in tumor-bearing versus naïve C57BL/6J mice ($n = 3$), suggesting that adaptive antitumor immunity was not generated by combination treatment (data not shown; mice were euthanized on day 120 after intracranial tumor inoculation). Interestingly, in the highly immunocompromised SCID NSG model, neither virus induced apoptosis in vivo (Supplementary Material, Fig. S13) nor provided a survival benefit in combination with TMZ (35 days for dead virus and 36.5 days, $P = .8$ for vMyxV-M011L-KO and TMZ combination, Fig. 4D).

We next investigated the effect of the combination treatment on apoptosis in immunocompetent mice utilizing immunohistochemistry staining of paraffin-embedded brain sections for cleaved caspase 3 and Ki-67 (Fig. 4E). In contrast to our in vitro data, vMyx-M011L-KO treatment alone did not result in robust caspase 3 activation in vivo when compared with vMyx-WT or UV-inactivated dead virus groups. However, the combination of vMyx-M011L-KO plus TMZ significantly increased the number of cleaved caspase 3-positive cells, compared with TMZ plus vMyx-WT or UV-inactivated virus (Supplementary Material, Fig. S14). In agreement with these data, a substantial decrease in tumor size was observed in brain sections from vMyx-M011L-KO and TMZ-treated mice. Together, these findings demonstrate the superior oncolytic efficacy of vMyx-M011L-KO in vivo, supporting the potential clinical utility of combined vMyx-M011L-KO and TMZ treatment.

Discussion

Many viruses modulate host survival pathways to override the cell's programmed cell death response and promote prolonged viral replication. Poxviruses encode various proteins that drive the host cell toward a permissive intracellular environment following infection.[32] We hypothesized that loss of antiapoptotic viral proteins would drive apoptosis following OV infection, thereby improving OV efficacy. Here, we report that deleting M011L triggers apoptosis of both human and murine BTICs following infection and extends survival of immunocompetent tumor-bearing mice in vivo (illustrated in Supplementary Material, Fig. S15). vMyx-WT suppresses a caspase 3/7-dependent apoptotic response in infected BTICs, as measured by caspase 3/7 activation, PARP cleavage, and cytochrome c release. This can be attributed to expression of the antiapoptotic viral protein M011L, which circumvents the programmed death response to viral infection through its interactions with Bak and Bax.[19,26,33] Despite the plethora of antiapoptotic proteins encoded by MYXV,[17] loss of M011L is sufficient to trigger apoptosis in infected BTICs. Since inducing tumor cell death is a primary goal of OV therapy, the induction of apoptosis by vMyx-M011L-KO increases its efficacy over WT virus. Further studies are needed to determine the mechanism by which the immune system mediates oncolytic efficacy of pro-apoptotic vMyx-M011L-KO in immunocompetent but not immunodeficient glioma models. One possibility is that innate immune effector cells secrete antitumor cytokines (eg, TNF-α or TRAIL) known to induce apoptosis and exhibit antitumor activities.[34] Reduced tumor burden and increased survival of tumor-bearing immunocompetent mice following vMyx-M011L-KO treatment is likely due to cell death induced both by vMyx-M011L-KO directly as well as immune mediators.

The observation that we are able to directly induce apoptosis in both human and murine BTIC models, when BTICs are classically considered to have heightened resistance to apoptosis,[35] is significant. Recent estimates by the Cancer Genome Atlas calculated that ∼87% of patients have alterations in p53 signaling, the quintessential pathway involved in apoptosis regulation.[36] We demonstrated that vMyx-M011L-KO is effective against both WT p53 (BTIC48) and p53 mutant (BTIC25) cells.[37] With the recent interest in proapoptotic therapies for gliomas, there are excellent opportunities to create synergy between a proapoptotic OV and targeted small molecule inhibitors. Given that other poxviruses (eg, vaccinia virus) are under development as OVs and that these viruses also encode homologs to Bcl-2, our strategy may be relevant to other OVs.

The development of an immunocompetent mBTIC model is important for assessing candidate glioblastoma therapeutics, since the immune system may be required for optimal treatment efficacy. OVs are increasingly recognized as inducers of immunologic antitumor responses, essentially acting as in situ tumor vaccines (reviewed in 6). It has also been found in a pancreatic cancer model that immune responses in syngeneic models are necessary for full antitumor efficacy of vMyx-WT.[24] This is only the second publication that has used a syngeneic BTIC line to test an OV; the first used a BTIC line derived from an activated H-ras and protein kinase B (Akt) model in $Tp53^{+/-}$ mice.[38,39] Our line (mBTIC0309) arose from NPcis C57BL/6J mice that spontaneously developed gliomas, which we cultured under standard neurosphere conditions.[4]

(C) Kaplan-Meier survival curve of mBTIC0309-bearing C57BL/6J mice treated with 5×10^6 FFUs of vMyx-WT, vMyx-M011L-KO, or UV-inactivated MYXV in combination with TMZ. Ten mice were randomly assigned to each experimental group, and a single intratumoral virus injection was performed on day 7 after tumor implantation. Half of the animals were treated with 100 mg/kg of TMZ (grey arrow) on day 10 after tumor implantation (day 3 after virus treatment) for 5 consecutive days. Statistical significance ($P < .007$, vMyx-M011L-KO compared with dead virus, and $P < .003$, combination of TMZ and vMyx-M011L-KO compared with combination of TMZ and dead virus) was determined using log-rank Mantel-Cox test. No statistical significance ($P = .8$) in median survival was observed in immunocompromised animals treated in combination with TMZ (D). The data represent results from at least 2 independent experiments with similar results. (E) Immunohistochemical analysis 14 days after tumor inoculation (7 days after MYXV and 5 days after TMZ treatment). The tumor size was reduced in vMyx-M011L-KO + TMZ group (VI). Scale bar 2 mm. Combination treatment with vMyx-M011L-KO, and TMZ led to significantly ($P < .05$, Supplementary Material, Fig. S14) stronger cleaved caspase 3 staining, indicating increased apoptotic cell death in vivo. Scale bar 200 μm. Slides shown are representative of similar observations in 2 different mice receiving same treatment regimen.

This line has many features of human glioblastomas and resembles the human disease histologically: it is invasive, vascular, has neuronal satellitosis, and expresses glioblastoma markers encountered in patient specimens. Our mBTIC line also retains stem cell characteristics when grown under neurosphere conditions: (i) it expresses stem cell markers CD-133, nestin, and Sox-2; and (ii) it can be induced with serum to express cell type-specific markers GFAP (astrocytes), Olig-2 (oligodendrocytes) and Tuji1 (neurons), suggesting multilineage differentiation. Because the mBTIC0309 parent tumor arose in an NPcis C57BL/6J mouse, this mBTIC line can be utilized in any WT or transgenic mice on a C57BL/6J background. Therefore, this is a widely applicable model for assessing potentially immunogenic glioblastoma therapies.

From our current study, it is evident that vMyx-M011L-KO with TMZ represents a highly effective OV-based regimen in high-grade brain tumor models. This regimen is being evaluated in additional preclinical models in our laboratories and is poised for clinical translation in glioma patients.

Supplementary Material

Supplementary material is available at *Neuro-Oncology Journal* online (http://neuro-oncology.oxfordjournals.org/).

Funding

Acknowledgments

Conflict of interest statement. The authors disclose no conflicts of interest.

References

1. Stupp R, Mason WP, van den Bent MJ, et al. Radiotherapy plus concomitant and adjuvant temozolomide for glioblastoma. *N Engl J Med*. 2005;352(10):987–996.

2. Singh SK, Hawkins C, Clarke ID, et al. Identification of human brain tumour initiating cells. *Nature*. 2004;432(7015):396–401.

3. Chen J, Li Y, Yu TS, et al. A restricted cell population propagates glioblastoma growth after chemotherapy. *Nature*. 2012; 488(7412):522–526.

4. Kelly JJ, Stechishin O, Chojnacki A, et al. Proliferation of human glioblastoma stem cells occurs independently of exogenous mitogens. *Stem Cells*. 2009;27(8):1722–1733.

5. Lee J, Kotliarova S, Kotliarov Y, et al. Tumor stem cells derived from glioblastomas cultured in bFGF and EGF more closely mirror the phenotype and genotype of primary tumors than do serum-cultured cell lines. *Cancer Cell*. 2006;9(5):391–403.

6. Chiocca EA, Blair D, Mufson RA. Oncolytic viruses targeting tumor stem cells. *Cancer Res*. 2014;74(13):3396–3398.

7. Lichty BD, Breitbach CJ, Stojdl DF, Bell JC. Going viral with cancer immunotherapy. *Nat Rev Cancer*. 2014;14(8):559–567.

8. Zemp FJ, Corredor JC, Lun X, Muruve DA, Forsyth PA. Oncolytic viruses as experimental treatments for malignant gliomas: using a scourge to treat a devil. *Cytokine Growth Factor Rev*. 2010; 21(2–3):103–117.

9. Zemp FJ, Lun X, McKenzie BA, et al. Treating brain tumor-initiating cells using a combination of myxoma virus and rapamycin. *Neuro Oncol*. 2013;15(7):904–920.

10. Lun X, Yang W, Alain T, et al. Myxoma virus is a novel oncolytic virus with significant antitumor activity against experimental human gliomas. *Cancer Res*. 2005;65(21):9982–9990.

11. Stanford MM, McFadden G. Myxoma virus and oncolytic virotherapy: a new biologic weapon in the war against cancer. *Expert Opin Biol Ther*. 2007;7(9):1415–1425.

12. McKenzie BA, Zemp FJ, Pisklakova A, et al. In vitro screen of a small molecule inhibitor drug library identifies multiple compounds that synergize with oncolytic myxoma virus against human brain tumor-initiating cells. *Neuro Oncol*. 2015;17(8):1086–1094.

13. Pareja F, Macleod D, Shu C, et al. PI3K and Bcl-2 inhibition primes glioblastoma cells to apoptosis through downregulation of Mcl-1 and phospho-BAD. *Mol Cancer Res*. 2014;12(7):987–1001.

14. Benedict CA, Norris PS, Ware CF. To kill or be killed: viral evasion of apoptosis. *Nat Immunol*. 2002;3(11):1013–1018.

15. Taylor JM, Barry M. Near death experiences: poxvirus regulation of apoptotic death. *Virology*. 2006;344(1):139–150.

16. Taylor RC, Cullen SP, Martin SJ. Apoptosis: controlled demolition at the cellular level. *Nat Rev Biol*. 2008;9(3):231–241.

17. Cameron C, Hota-Mitchell S, Chen L, et al. The complete DNA sequence of myxoma virus. *Virology*. 1999;264(2):298–318.

18. Douglas AE, Corbett KD, Berger JM, McFadden G, Handel TM. Structure of M11L: A myxoma virus structural homolog of the apoptosis inhibitor, Bcl-2. *Protein Sci*. 2007;16(4):695–703.

19. Everett H, Barry M, Sun X, et al. The myxoma poxvirus protein, M11L, prevents apoptosis by direct interaction with the mitochondrial permeability transition pore. *J Exp Med*. 2002; 196(9):1127–1139.

20. Wang G, Barrett JW, Nazarian SH, et al. Myxoma virus M11L prevents apoptosis through constitutive interaction with Bak. *J Virol*. 2004;78(13):7097–7111.

21. Reilly KM, Loisel DA, Bronson RT, McLaughlin ME, Jacks T. Nf1;Trp53 mutant mice develop glioblastoma with evidence of strain-specific effects. *Nat Genet*. 2000;26(1):109–113.

22. Reilly KM, Tuskan RG, Christy E, et al. Susceptibility to astrocytoma in mice mutant for Nf1 and Trp53 is linked to chromosome 11 and subject to epigenetic effects. *Proc Natl Acad Sci USA*. 2004; 101(35):13008–13013.

23. Opgenorth A, Graham K, Nation N, Strayer D, McFadden G. Deletion analysis of two tandemly arranged virulence genes in myxoma virus, M11L and myxoma growth factor. *J Virol*. 1992;66(8): 4720–4731.

24. Wennier ST, Liu J, Li S, Rahman MM, Mona M, McFadden G. Myxoma virus sensitizes cancer cells to gemcitabine and is an effective oncolytic virotherapeutic in models of disseminated pancreatic cancer. *Mol Ther*. 2012;20(4):759–768.

25. Smallwood SE, Rahman MM, Smith DW, McFadden G. Myxoma virus: propagation, purification, quantification, and storage. *Curr Protoc Microbiol*. 2010;17:14A.1.1–14A.1.20.

26. Everett H, Barry M, Lee SF, et al. M11L: a novel mitochondria-localized protein of myxoma virus that blocks apoptosis of infected leukocytes. *J Exp Med*. 2000;191(9):1487–1498.

27. Nechushtan A, Smith CL, Hsu YT, Youle RJ. Conformation of the Bax C-terminus regulates subcellular location and cell death. *EMBO J*. 1999;18(9):2330–2341.

28. Cuvillier O, Nava VE, Murthy SK, et al. Sphingosine generation, cytochrome c release, and activation of caspase-7 in doxorubicin-induced apoptosis of MCF7 breast adenocarcinoma cells. *Cell Death Differ*. 2001;8(2):162–171.

29. Shultz LD, Lyons BL, Burzenski LM, et al. Human lymphoid and myeloid cell development in NOD/LtSz-scid IL2R gamma null mice engrafted with mobilized human hemopoietic stem cells. *J Immunol*. 2005;174(10):6477–6489.

30. Ishikawa F, Yasukawa M, Lyons B, et al. Development of functional human blood and immune systems in NOD/SCID/IL2 receptor {gamma} chain(null) mice. *Blood*. 2005;106(5):1565–1573.

31. Popa N, Cedile O, Pollet-Villard X, Bagnis C, Durbec P, Boucraut J. RAE-1 is expressed in the adult subventricular zone and controls cell proliferation of neurospheres. *Glia*. 2011;59(1):35–44.

32. Everett H, McFadden G. Viruses and apoptosis: meddling with mitochondria. *Virology*. 2001;288(1):1–7.

33. Kvansakul M, van Delft MF, Lee EF, et al. A structural viral mimic of prosurvival Bcl-2: a pivotal role for sequestering proapoptotic Bax and Bak. *Mol Cell*. 2007;25(6):933–942.

34. Calzascia T, Pellegrini M, Hall H, et al. TNF-alpha is critical for antitumor but not antiviral T cell immunity in mice. *J Clin Invest*. 2007;117(12):3833–3845.

35. Kruyt FA, Schuringa JJ. Apoptosis and cancer stem cells: Implications for apoptosis targeted therapy. *Biochem Pharmacol*. 2010;80(4):423–430.

36. Cancer Genome Atlas Research N. Comprehensive genomic characterization defines human glioblastoma genes and core pathways. *Nature*. 2008;455(7216):1061–1068.

37. Blough MD, Beauchamp DC, Westgate MR, Kelly JJ, Cairncross JG. Effect of aberrant p53 function on temozolomide sensitivity of glioma cell lines and brain tumor initiating cells from glioblastoma. *J Neurooncol*. 2011;102(1):1–7.

38. Marumoto T, Tashiro A, Friedmann-Morvinski D, et al. Development of a novel mouse glioma model using lentiviral vectors. *Nat Med*. 2009;15(1):110–116.

39. Cheema TA, Wakimoto H, Fecci PE, et al. Multifaceted oncolytic virus therapy for glioblastoma in an immunocompetent cancer stem cell model. *Proc Natl Acad Sci USA*. 2013;110(29): 12006–12011.